

Project acronym:	GeoSmart		
Project title:	Technologies for geothermal to enhance competitiveness in smart and flexible operation		
Activity:	LC-SC3-RES-12-2018		
Call:	H2020-LC-SC3-2018-RES-SingleStage		
Funding Scheme:	IA	Grant Agreement No	818576
	WP 4	Development of scaling reduction system	

D4.1 –Modelling of silica scaling potential

Due date:	31/05/2020 (M12)		
Actual Submission Date:	28/05/2020		
Lead Beneficiary:	Uol		
Main authors/contributors:	Uol		
Dissemination Level¹:	PU		
Nature:	REPORT		
Status of this version:		Draft under Development	
		For Review by Coordinator	
	X	Submitted	
Version:	2		
Abstract	This deliverable reports on the mathematical modelling of silica scaling potential.		

REVISION HISTORY

Version	Date	Main Authors/Contributors	Description of changes
V1	26.05.2020	Uol, ON, Zorlu, Gerosion, ON	
V2	28.05.2020	Uol, ON, Zorlu, Gerosion, ON, TWI	Text revisions



This project has received funding from the *European Union's Horizon 2020 research and innovation programme* under grant agreement No 818576

¹ Dissemination level security:

PU – Public (e.g. on website, for publication etc.) / **PP** – Restricted to other programme participants (incl. Commission services) /

RE – Restricted to a group specified by the consortium (incl. Commission services) / **CO** – confidential, only for members of the consortium (incl. Commission services)

This project has received funding from the European Union's Horizon 2020 program Grant Agreement No 818576. This publication reflects the views only of the author(s), and the Commission cannot be held responsible for any use which may be made of the information contained therein.

Copyright © 2019-2023, GeoSmart Consortium

This document and its contents remain the property of the beneficiaries of the GeoSmart Consortium and may not be distributed or reproduced without the express written approval of the GeoSmart Coordinator, TWI Ltd. (www.twi-global.com)

THIS DOCUMENT IS PROVIDED BY THE COPYRIGHT HOLDERS AND CONTRIBUTORS "AS IS" AND ANY EXPRESS OR IMPLIED WARRANTIES, INCLUDING, BUT NOT LIMITED TO, THE IMPLIED WARRANTIES OF MERCHANTABILITY AND FITNESS FOR A PARTICULAR PURPOSE ARE DISCLAIMED. IN NO EVENT SHALL THE COPYRIGHT OWNER OR CONTRIBUTORS BE LIABLE FOR ANY DIRECT, INDIRECT, INCIDENTAL, SPECIAL, EXEMPLARY, OR CONSEQUENTIAL DAMAGES (INCLUDING, BUT NOT LIMITED TO, PROCUREMENT OF SUBSTITUTE GOODS OR SERVICES; LOSS OF USE, DATA, OR PROFITS; OR BUSINESS INTERRUPTION) HOWEVER CAUSED AND ON ANY THEORY OF LIABILITY, WHETHER IN CONTRACT, STRICT LIABILITY, OR TORT (INCLUDING NEGLIGENCE OR OTHERWISE) ARISING IN ANY WAY OUT OF THE USE OF THIS DOCUMENT, EVEN IF ADVISED OF THE POSSIBILITY OF SUCH DAMAGE.

CONTENTS

1	EXECUTIVE SUMMARY.....	4
2	OBJECTIVES MET.....	5
3	INTRODUCTION.....	5
4	THERMODYNAMICS AND SOLUBILITY OF AQUEOUS SILICA.....	7
4.1	SILICA IONSATION AND COMPLEXATION REACTIONS	7
4.2	SILICA (SiO _{2(s)}) SOLID SOLUBILITY.....	8
5	SILICA POLYMERISATION.....	13
5.1	MECHANISM AND RATE OF SILICA POLYMERISATION AND PRECIPITATION.....	13
5.2	RATE OF SILICA POLYMERISATION.....	14
6	TEST OF SILICA POLYMERISATION UNDER GEOTHERMAL RELEVANT CONDITIONS	19
6.1	OVERVIEW.....	19
6.2	GEOTHERMAL FIELDS AND SCALING ISSUES.....	19
6.2.1	Kizildere.....	19
6.2.2	Nesjavellir.....	20
6.2.3	Hellisheiði.....	21
6.3	EXPERIMENTAL TESTS.....	22
6.3.1	Overview.....	22
6.3.2	Methods	23
6.3.3	Results and discussion.....	24
7	CONCLUSIONS.....	26
	REFERENCES.....	27

1 EXECUTIVE SUMMARY

Aqueous silica ($\text{SiO}_{2(\text{aq})}$) is among major elements in geothermal fluids with typical concentrations between ~100-1000 ppm in low- to high-enthalpy geothermal systems. Upon cooling associated with depressurisation boiling and conductive cooling, particularly at lower temperatures (<100°C) geothermal waters typically become supersaturated with amorphous silica (AM silica) that may precipitate to form silica scales. To prevent silica scaling within geothermal infrastructure (wellheads, pipelines, separators and re-injection boreholes), high (120-180°C) utilisation and re-injection temperatures are commonly employed instead of utilisation to lower temperatures.

The mechanism of silica scaling involves aqueous silica polymerisation, i.e. stepwise reaction of monomeric silica (one Si atom compound) to form polymer chains and three-dimensional networks (two and more Si atom compounds) followed by transformation of the polymers into precipitate through the mechanism of ripening, aggregation (coagulation, flocculation), and cementation. The initial step and maximum rate of silica scaling is, therefore, commonly taken as the rate of aqueous silica polymerisation.

According to molecular simulations, the polymerisation of aqueous silica is described by stepwise addition of aqueous monomeric silica to form linear di-, tri- and tetramers and cyclic tri- and tetramers. Further aqueous silica polymerisation is not energetically favorable. It follows that the rate of aqueous silica polymerisation may be described by a fourth order reaction that available literature data were fitted to in order to obtain a mathematical function describing the rate of aqueous silica polymerisation at ~25-80°C, pH ~3-10 and ionic strength $I < 0.2$ molal,

$$\frac{dm_{\text{SiO}_{2(\text{aq})}}}{dt} = -k \left(m_{\text{SiO}_{2(\text{aq})}} - m_{\text{SiO}_{2(\text{aq}),\text{eq}}} \right)^4$$

and

$$k = A \exp(-E_a/RT) a_{\text{H}_4\text{SiO}_4,\text{aq}}^3 a_{\text{H}^+}^{-0.75}$$

where k is the rate constant, $m_{\text{SiO}_{2(\text{aq})}}$ and $m_{\text{SiO}_{2(\text{aq}),\text{eq}}}$ are aqueous monomeric silica in solution and AM silica equilibrium concentration, A is the pre-exponential factor of $(3.95 \pm 1.16) \cdot 10^6$, E_a is the activation energy with value of 13.9 ± 9.8 kJ, T and R are temperature and the gas constant, and $a_{\text{H}_4\text{SiO}_4,\text{aq}}$ and a_{H^+} are the activities of aqueous $\text{H}_4\text{SiO}_4(\text{aq})$ and H^+ species. Using the obtained rate function, it can be concluded that the rate of aqueous silica polymerisation and silica scaling is at maximum at pH ~8-9 and decreases with decreasing and increasing pH, increases with increasing initial $\text{SiO}_{2(\text{aq})}$ concentration, and increases with increasing temperature.

The obtained rate function was validated against experimental tests on aqueous silica polymerisation upon cooling of synthetic geothermal fluids similar to those observed at Kizildere II (Turkey), Nesjavellir (Iceland) and Hellisheiði (Iceland) power plants. A reasonably good comparison was observed in all cases. Based on these tests, and using the rate function, it can be concluded that cooling of the re-injection water at Kizildere-II to 70°C results in insignificant aqueous silica polymerisation and further cooling to 40°C may result in minor $\text{SiO}_{2(\text{aq})}$ polymerisation (~1% after 10 minutes and ~5% after 60 minutes). In contrast, cooling of waters at Nesjavellir and Hellisheiði that contain up to 800 ppm of $\text{SiO}_{2(\text{aq})}$ to 80°C will result in significant $\text{SiO}_{2(\text{aq})}$ polymerisation within minutes (~25% within 10 minutes and ~40% within an hour). Further cooling will enhance the polymerisation (>50% within 10 minutes at 23-58°C). Upon mixing of such brines with condensed steam aqueous silica polymerisation rates are greatly reduced due to dilution and decreased rate with decreasing pH.

2 OBJECTIVES MET

The deliverable contributes to the general aim of the work package's objectives:

- Technology transfer developments for designing and optimising the scaling-reduction system for the Zorlu KZD1 demonstrator, based on the Icelandic experiences.
- To extend the knowledgebase for design and operation of this and generic silica systems, and to evaluate the effects on reservoir sustainability of the increased enthalpy removal. In this work package, we will demonstrate a scale reduction system that enables re-injection temperatures down to around 50 °C, thereby almost doubling the extractable heat energy by allowing for $t=96^{\circ}\text{C}$

The major focus of the document was to define initial information related to optimisation and design of the scaling-reduction system:

- Assessing chemistry of the geothermal working fluid (brine) at demonstration sites.
- Development of mathematical model that describes silica polymerisation rate and reaction mechanism under geothermal conditions and based on literature data.
- Small scale laboratory testing of the results of the mathematical modelling.

3 INTRODUCTION

Dissolved silica ($\text{SiO}_{2(\text{aq})}$) is among major elements in geothermal waters sourced from dissolution of silica bearing minerals by the geothermal fluids. For low- and medium enthalpy fluids ($<150^{\circ}\text{C}$, $h>1000$ kJ/kg), the $\text{SiO}_{2(\text{aq})}$ concentrations are usually low or <300 ppm whereas for high-enthalpy fluids ($>200^{\circ}\text{C}$) $\text{SiO}_{2(\text{aq})}$ concentrations can range between ~ 400 and 1000 ppm. The concentration of $\text{SiO}_{2(\text{aq})}$ in such high-enthalpy reservoir geothermal waters is considered to be controlled by equilibrium between dissolved monomeric silica ($\text{H}_4\text{SiO}_{4(\text{aq})}$) and the quartz mineral ($\text{SiO}_{2(\text{s})}$). The solubility of quartz and other silica oxides minerals like chalcedony and amorphous silica (AM silica) increase with increasing temperature. It also depends on pH as $\text{H}_4\text{SiO}_{4(\text{aq})}$ can ionise and form ion-pairs increasing the solubility of solid silica dioxide. During the ascent of high temperature geothermal fluid from the reservoirs to the surface and during its utilisation it cools down and water becomes supersaturated with respect to quartz and therefore it has a potential to form. By experience, quartz does not form upon cooling of geothermal water, instead, fluid that has high silica content (>300 - 400 ppm $\text{SiO}_{2(\text{aq})}$) reach AM silica supersaturation resulting in $\text{SiO}_{2(\text{aq})}$ polymerisation and possibly AM silica deposition and/or scaling (Figure 1). The rate of $\text{SiO}_{2(\text{aq})}$ polymerisation is fast in supersaturated solutions, on the orders of minutes to hours, and is considered to depend on initial $\text{SiO}_{2(\text{aq})}$ concentration, pH, temperature and ionic strength (e.g. Carroll et al., 1998; Icopini et al., 2005; Tobler and Benning, 2013).

The standard method for preventing silica scaling is to limit the utilisation to high-enough temperatures to prevent supersaturation of AM silica or to ~ 100 - 180°C depending on the initial $\text{SiO}_{2(\text{aq})}$ concentration followed by re-injection into the geothermal reservoir. Several other methods have also been utilised to prevent silica scaling in geothermal boreholes and pipelines including:

- The geothermal wastewater pH modification (e.g. Gill, 1993; Gudmundsson and Einarsson, 1989).
- Mixing with water of low $\text{SiO}_{2(\text{aq})}$ concentration or dilution for example steam condensate (e.g. Gallup and Featherstone, 1985).
- Addition of organic inhibitors (e.g. Gallup, 1998; Candelaria et al., 1996).
- Controlled precipitation by introducing a silica gel into the water (e.g. Sugita et al., 1998; 1999).
- Addition of cationic reactant to trigger silica deposition (e.g. Ueda et al., 2000; 2003).
- Storage in a retention ponds or tanks (e.g. Yanagase et al., 1970; Gunnarsson et al., 2010).

These methods have proven successful in individual geothermal fields but they are not universal.

When geothermal waters become supersaturated with AM silica two kinds of processes may take place:

- Polymerisation of dissolved aqueous silica.
- AM silica deposition (scaling) onto surfaces.

The silica polymerisation reactions involve reactions of monomeric silica to form polymers containing two or more silica atoms. Following this, the polymers can aggregate to form clusters of AM silica. This process can either occur in solution or on surfaces forming AM silica deposits and scales (Figure 2; Tobler and Benning, 2013; van den Heuvel et al., 2018). Which process takes place is not well understood but depends on various chemical and physical factors like degree of water supersaturation with respect to AM silica and type of fluid flow.

The rate of silica polymerisation has been studied over a wide range of temperature and solution compositions, and depends on factors like the initial $\text{SiO}_{2(\text{aq})}$ concentration, pH, temperature and ionic strength. However, laboratory rates of $\text{SiO}_{2(\text{aq})}$ polymerisation do not necessarily reflect rates of silica scale deposition observed in the field (Carroll et al., 1998; van den Heuvel et al., 2018). This makes it difficult to accurately predict silica scaling and has led to the practice that silica scaling problems are usually solved using site-specific field solutions for a given geothermal installation or more general avoided by high fluid re-injection temperatures to avoid AM silica scale formation. However, initial and maximum AM silica scaling rates may be assumed to correspond to aqueous silica polymerisation rates. It follows that actual field rates of AM silica scaling are equivalent or slower than the $\text{SiO}_{2(\text{aq})}$ polymerisation rates.

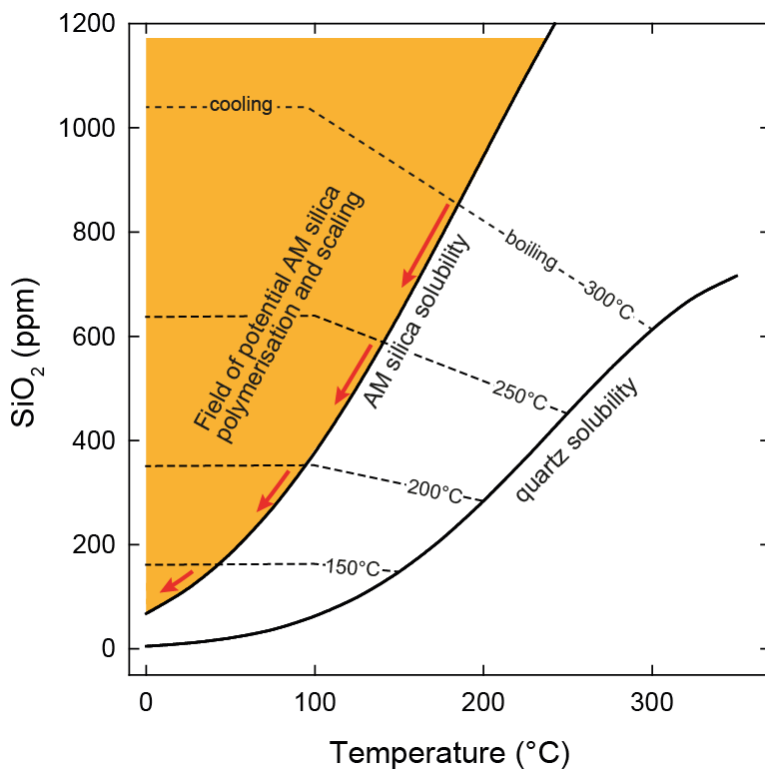


Figure 1. The solubility of quartz and AM silica in geothermal water (solid lines, Table 3) and AM silica scaling potential. The dashed lines represent the geothermal water initially in equilibrium with quartz followed by isoenthalpic boiling to 100°C and conductive cooling. The orange coloured field represents conditions where the water become supersaturated with respect to AM silica and $\text{SiO}_{2(\text{aq})}$ polymerisation and scaling may occur.

In this report the thermodynamics and solubility of silica in geothermal water is summarised, available data on the rates of silica polymerisation are reviewed and a uniform rate equation for geothermal application developed. This equation is then compared with the results of the tests simulating silica polymerisation upon temperature decrease during utilisation of geothermal fluids from Kizildere (Turkey), Hellisheiði and Nesjavellir (Iceland). As a result, the potential for silica scaling in real geothermal fluids was assessed.

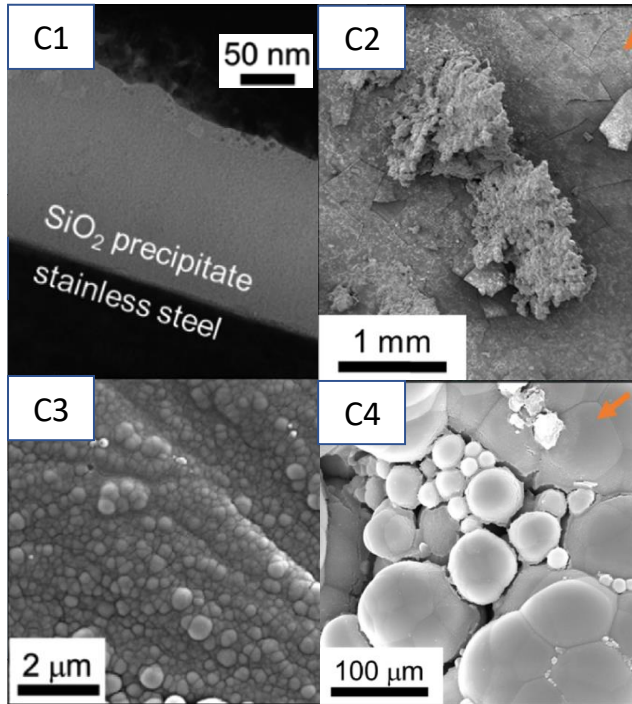


Figure 2. Scanning electron microscope (SEM) images show silica scales and aggregates. C1: layer of silica scales on a stainless steel surface; C2: spherical silica aggregates that grew as a function of time seemingly by addition of individual particles that were then cemented together; C3: AM silica on the surface of a stainless steel plate; C4: AM silica growth bumps that have merged together. From van den Heuvela et al. (2018)

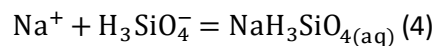
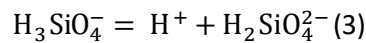
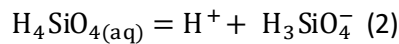
4 THERMODYNAMICS AND SOLUBILITY OF AQUEOUS SILICA

4.1 Silica ionisation and complexation reactions

Dissolved aqueous silica ($\text{SiO}_{2(\text{aq})}$) may form different monomeric (single Si atom) compounds (aqueous species) including $\text{H}_4\text{SiO}_{4(\text{aq})}$, H_3SiO_4^- , $\text{H}_2\text{SiO}_4^{2-}$ and $\text{NaH}_3\text{SiO}_{4(\text{aq})}$. The total concentration of $\text{SiO}_{2(\text{aq})}$ in water corresponds to the sum of the concentrations of these aqueous species:

$$m_{\text{SiO}_{2(\text{aq})}} = m_{\text{H}_4\text{SiO}_{4(\text{aq})}} + m_{\text{H}_3\text{SiO}_4^-} + m_{\text{H}_2\text{SiO}_4^{2-}} + m_{\text{NaH}_3\text{SiO}_4} \quad (1)$$

Where m is the molal (mol/kg) concentration. The relationship between the aqueous species is described by the corresponding reactions



and their equilibrium constants

$$K_1 = \frac{a_{\text{H}_3\text{SiO}_4^-} \cdot a_{\text{H}^+}}{a_{\text{H}_4\text{SiO}_{4(\text{aq})}}} = \frac{m_{\text{H}_3\text{SiO}_4^-} \cdot m_{\text{H}^+}}{m_{\text{H}_4\text{SiO}_{4(\text{aq})}}} \cdot \frac{\gamma_{\text{H}_3\text{SiO}_4^-} \cdot \gamma_{\text{H}^+}}{\gamma_{\text{H}_4\text{SiO}_{4(\text{aq})}}} \quad (5)$$

$$K_2 = \frac{a_{\text{H}_2\text{SiO}_4^{2-}} \cdot a_{\text{H}^+}}{a_{\text{H}_3\text{SiO}_4^-}} = \frac{m_{\text{H}_2\text{SiO}_4^{2-}} \cdot m_{\text{H}^+}}{m_{\text{H}_3\text{SiO}_4^-}} \cdot \frac{\gamma_{\text{H}_2\text{SiO}_4^{2-}} \cdot \gamma_{\text{H}^+}}{\gamma_{\text{H}_3\text{SiO}_4^-}} \quad (6)$$

$$K_3 = \frac{a_{NaH_3SiO_4(aq)}}{a_{H_3SiO_4^-} \cdot a_{Na^+}} = \frac{m_{NaH_3SiO_4(aq)}}{m_{H_3SiO_4^-} \cdot m_{Na^+}} \cdot \frac{\gamma_{NaH_3SiO_4(aq)}}{\gamma_{H_3SiO_4^-} \cdot \gamma_{Na^+}} \quad (7)$$

where a and γ is the aqueous species activity and activity coefficient respectively, and K is the equilibrium constant. The aqueous species activity coefficients may be calculated using the Davies or equation

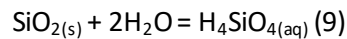
$$-\log\gamma = -0.5z^2 \left(\frac{\sqrt{I}}{1+\sqrt{I}} - 0.3I \right) \quad (8)$$

where z is the ion charge and I is the ionic strength. The aqueous H^+ activity is related to pH through the relationship $pH = -\log a_{H^+}$. It follows that the individual concentration of aqueous silica species can be calculated by solving the above equations.

The values of the equilibrium constants have been experimentally determined over a wide range of temperature (Table 1). These were fitted to an extended temperature function to generate smoothed equilibrium constants over the temperature range of interest in geothermal applications (Table 3). The experimental and obtained smoothed functions are compared in Figure 3.

4.2 Silica ($SiO_{2(s)}$) solid solubility

The solubility of solid silica ($SiO_{2(s)}$) may be described by the reaction and the corresponding equilibrium constant,



$$K = m_{H_4SiO_{4(aq)}} \quad (10)$$

The values of the equilibrium constants have been experimentally determined over a wide range of temperature (Table 2). These have been previously fitted to an extended temperature function to generate smoothed equilibrium constants over the temperature range of interest in geothermal applications (Gunnarsson and Arnórsson, 2000, Table 3). The experimental and obtained smoothed function for AM-silica and quartz are compared in Figure 4.

The solubility is further affected by the increasing activity of $H_3SiO_4^-$, $H_2SiO_4^{2-}$ and $NaH_3SiO_4(aq)$ and decreasing activity of $H_4SiO_4(aq)$ with increasing pH at a given temperature. An example of AM-silica solubility using the data presented in Table 3 is given in Figure 5 at 25 and 100° C.

Table 1 Hydrolysis and ion-pair constants for $\text{SiO}_{2(\text{aq})}$ at water vapor saturation pressure

Reactions	Range	Reference	
$\text{H}_4\text{SiO}_{4(\text{aq})} = \text{H}^+ + \text{H}_3\text{SiO}_4^-$	25-35°C	Greenberg and Price (1957)	
	25°C	Schwarz and Muller (1958)	
	20°C	Greenberg (1958)	
	25-50°C, 0.5-3M NaClO ₄	Lagerstrom (1959)	
	25, 0.5M NaCl	Inqri (1959)	
	346-364°C	Vilim (1961)	
	25, 0.5M NaClO ₄	Bilinski and Ingri (1967)	
	25-250°C	Ryzhenko (1967)	
	130-350°C, 0-0.6m NaCl	Seward (1974)	
	50-300°C, 0.1-5.0m NaCl	Busey and Mesmer. (1977)	
	25°C, 0.6M NaCl	Sjöberg et al. (1981)	
$\text{H}_4\text{SiO}_{4(\text{aq})} = 2\text{H}^+ + \text{H}_2\text{SiO}_4^{2-}$	25, 0.5M NaCl	Inqri (1959)	
	25-50°C, 0.5-3M NaClO ₄	Lagerstrom (1959)	
	25-250°C	Ryzhenko (1967)	
	025-350°C	Naumov et al. (1971)	
	25°C, 0.6M NaCl	Sjöberg et al. (1981)	
$\text{Na}^+ + \text{H}_3\text{SiO}_4^- = \text{NaH}_3\text{SiO}_4(\text{aq})$	130-350°C, 0-0.6m NaCl	Seward (1974)	

Table 2 Solubility determination of AM silica and quartz at water vapor saturation pressure

Mineral	Range	Reference	
AM silica	90°C	Lenher and Merrill (1917)	
	128-336°C	Hitchen (1935)	
	25°C	Alexander (1954)	
	25°C	Greenberg and Price (1957)	
	36-95°C	Elmer and Nordberg (1958)	
	0-100°C	Kitahara (1960)	
	25-90°C	Siever (1962)	
	25°C	Morey et al. (1964)	
	25-300°C	Marshall (1980)	
	100-350°C	Chen and Marshall (1982)	
	8-310°C	Gunnarsson and Arnórsson (2000)	
Quartz	160-379°C	Kennedy (1950)	
	140-370°C	Kitahara (1960)	
	69-240°C	Morey et al. (1962)	
	60-100°C	van Lier et al. (1960)	
	125-140°C	Siever (1962)	
	179-329°C	Crerar and Anderson (1971)	
	20°C	MacKenzie and Gees (1971)	
		Hemley et al. (1980)	
	21-96°C	Rimstidt (1997)	

Table 3 Smoothed equilibrium functions for $\text{SiO}_{2(\text{aq})}$ species and silica mineral solubilities. Valid at 0-350°C and water vapor saturation pressure

Reaction	$\log K = a + bT + c/T + d/T^2 + eT^2 + f \log T$					
	a	b	c	d	e	f
$\text{H}_4\text{SiO}_4(\text{aq}) = \text{H}^+ + \text{H}_3\text{SiO}_4^-$ ^a	6442.75	1.87823	-275914	12800171	-6.112E-04	-2496.26
$\text{H}_4\text{SiO}_4(\text{aq}) = 2\text{H}^+ + \text{H}_2\text{SiO}_4^{2-}$ ^a	-9785.05	-2.68970	429602	-21597490	7.859E-04	3757.15
$\text{Na}^+ + \text{H}_3\text{SiO}_4^- = \text{NaH}_3\text{SiO}_4(\text{aq})$ ^b			270		2.710E-06	
$\text{quartz} + 2\text{H}_2\text{O} = \text{H}_4\text{SiOH}_4(\text{aq})$ ^c	-34.188		197.47		-5.851E-06	12.245
$\text{AM-silica} + 2\text{H}_2\text{O} = \text{H}_4\text{SiOH}_4(\text{aq})$ ^c	-8.476		-485.24		-2.268E-06	3.068
$\text{calcedony} + 2\text{H}_2\text{O} = \text{H}_4\text{SiOH}_4(\text{aq})$ ^b	0.11		-1101			
$\text{cristobalite} + 2\text{H}_2\text{O} = \text{H}_4\text{SiO}_4(\text{aq})$ ^c	-35.575		391.75		-6.119E-06	12.712
^a This study						
^b Arnórsson et al. (1982)						
^c Gunnarsson and Arnórsson (2000)						

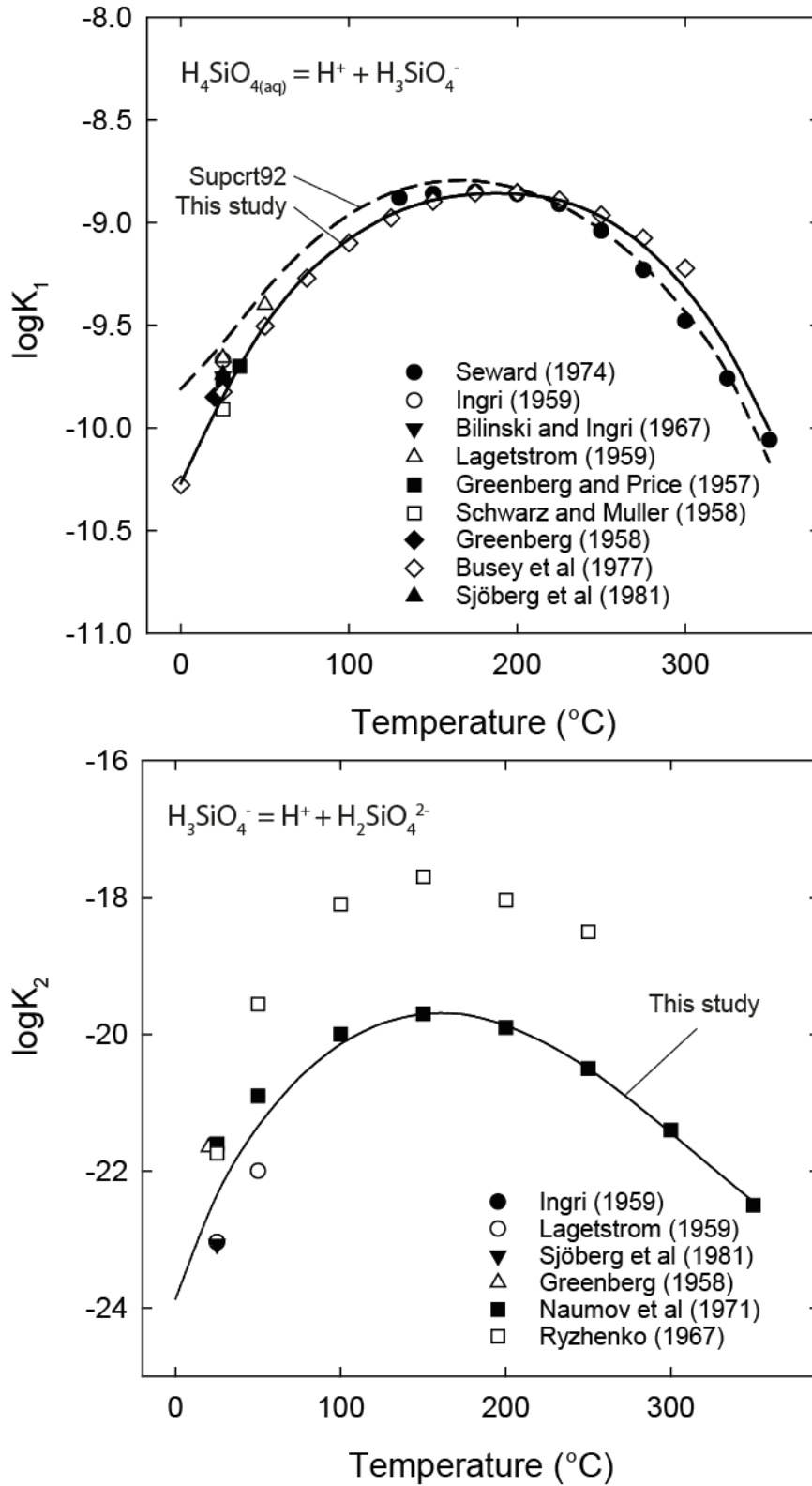


Figure 3. Aqueous silica species equilibrium constants as a function of temperature.

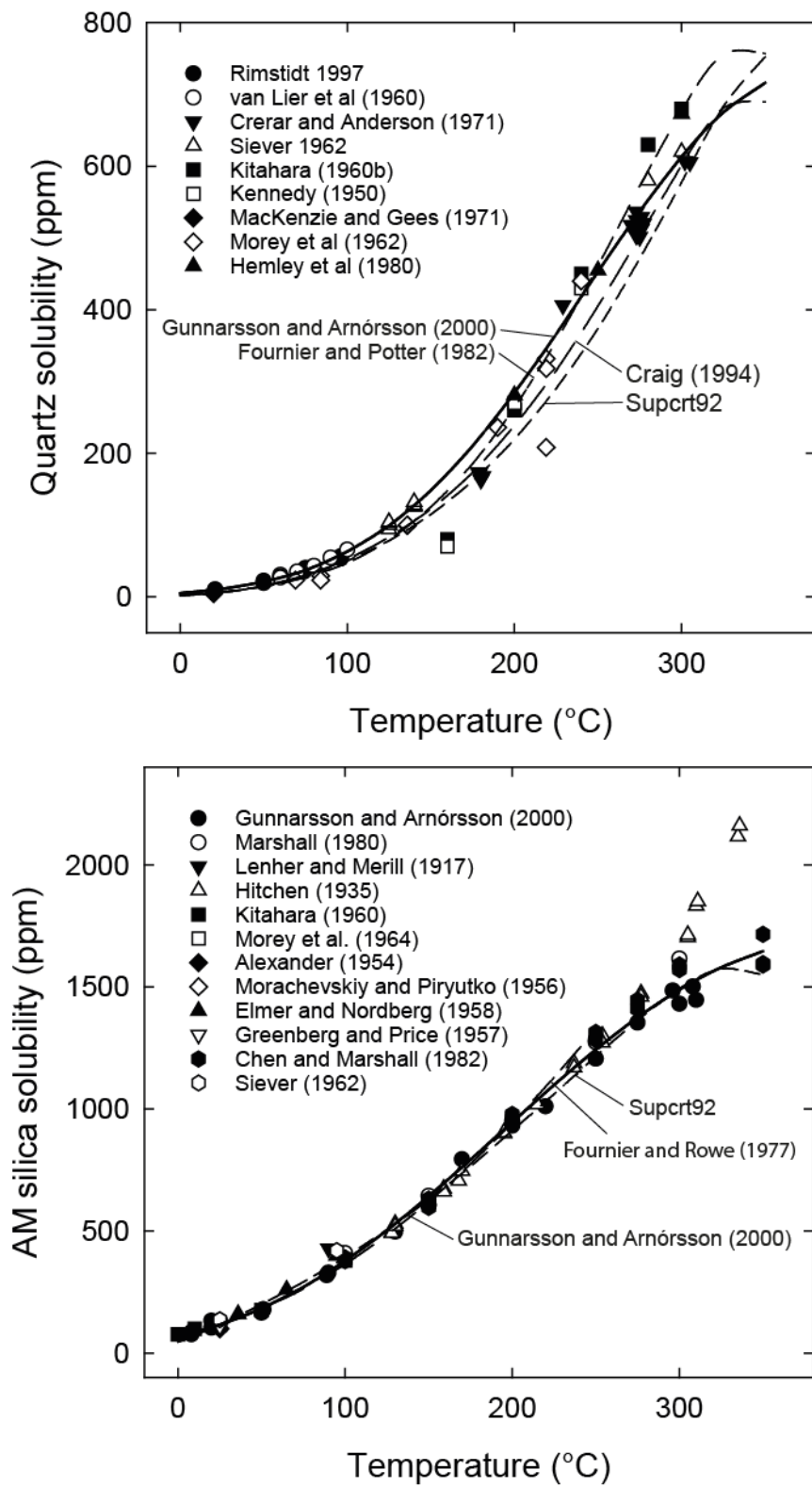


Figure 4. AM silica and quartz solubility as a function of temperature.

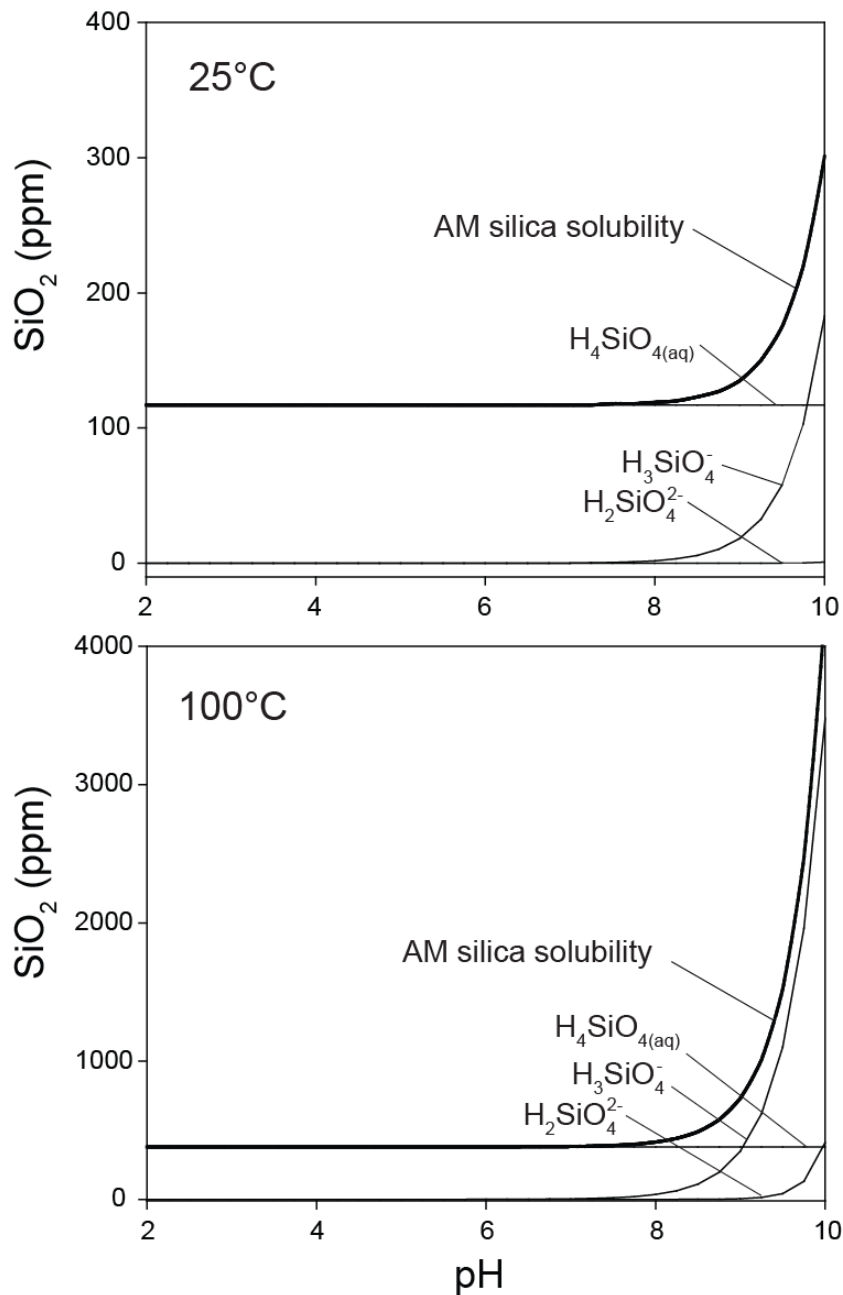


Figure 5. The solubility of AM-silica as a function of pH at 25 and 100°C and ionic strength of 0.01 m NaCl together with the dominant aqueous silica species in solution. Note the solubility is independent of pH to ~8-9 followed by sharp increase in solubility with increasing pH and that the solubility increases ca 10x between 25 and 100°C.

5 SILICA POLYMERISATION

5.1 Mechanism and rate of silica polymerisation and precipitation

When geothermal waters become supersaturated with AM silica two kinds of processes may take place: (1) polymerisation of dissolved SiO_{2(aq)} and (2) AM silica deposition (scaling) directly onto surfaces. In the initial step of the polymerisation often referred to as oligomerisation, the dissolved aqueous silica reacts to form dimers to hexamers (oligomers with 2-6 monomeric units). Following this, fast and spontaneous growth by monomer and dimer addition leads to formation of nanocolloidal particles (e.g. Conrad et al., 2007; Tobler et al., 2009). The transformation of the nanocolloidal particles to precipitates requires their ripening, aggregation (coagulation, flocculation), and cementation that happens before completing ripening process (Benning et al., 2007; Conrad et al., 2007; Icopini et al., 2005; Wen et al., 2020) (Figure 2). The step of SiO_{2(aq)} polymerisation

may be regarded as the initial stage of AM silica scaling; if the rate of $\text{SiO}_{2(\text{aq})}$ polymerisation is slower than the retention time of $\text{SiO}_{2(\text{aq})}$ in a given installation then AM silica scaling potential is negligible.

According to the result of recent molecular simulations, the polymerisation of $\text{SiO}_{2(\text{aq})}$ can be described by stepwise addition of monomeric $\text{SiO}_{2(\text{aq})}$ to form linear di-, tri- and tetramers. The linear tri- and tetramers can then further evolve to form cyclic tri- and tetramers (Figure 6; Zhang et al., 2011; Ciantar et al., 2015). The cyclic tetramer (ring structure of Si-O) has been proposed to be the end-product, the polymerisation mostly stops, and these units start to agglomerate to form scales. It should be noted that the cyclic tetramer is very common in various Si-containing solids in nature, for example in zeolites. The various polymerisation steps have been predicted to depend on availability of H_3SiO_4^- ($\text{Si}(\text{OH})_3\text{O}^-$) that “attach” Si-OH bond on $\text{H}_4\text{SiO}_4(\text{aq})$ ($\text{Si}(\text{OH})_4$) to form linear dimer, trimer and tetramer with bridging Si-O-Si groups. With increasing pH the availability of H_3SiO_4^- and hence the rate of polymerisation increases with increasing pH. In contrast, at more alkaline pH the availability of H_4SiO_4 decreases due to ionisation and therefore the rate of polymerisation decreases.

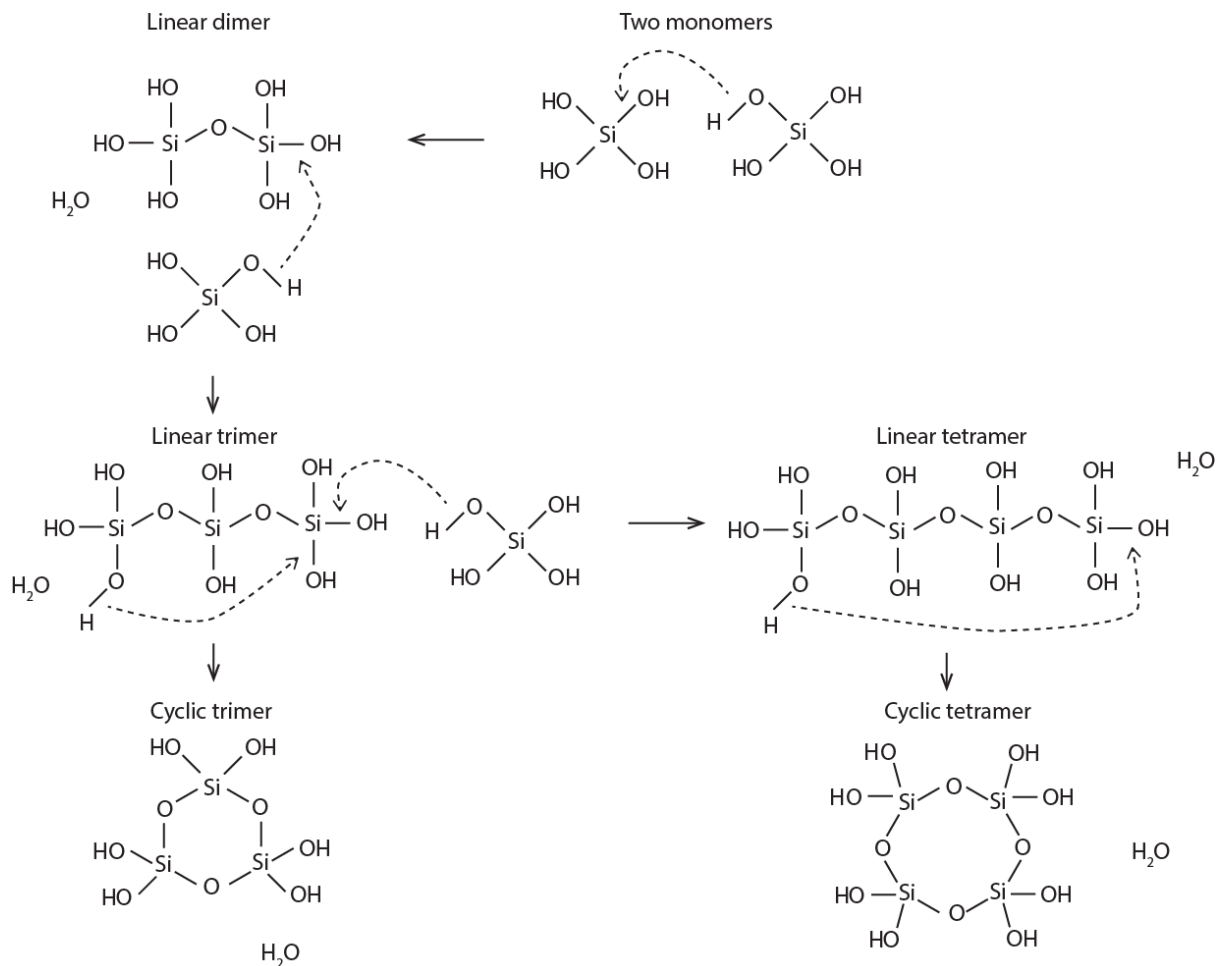


Figure 6. Schematic figure of the mechanism of silica polymerisation in aqueous solution according to recent theoretical simulations (based on Zhang et al., 2011; Ciantar et al. 2015)

5.2 Rate of silica polymerisation

The kinetic models describing silica polymerisation and precipitation have been derived from the measurements of decrease in monomeric $\text{SiO}_{2(\text{aq})}$ concentrations in solutions supersaturated with respect to AM silica with time. A summary of previous work is on kinetics of polymerisation is given in Table 4. The various studies span a wide range of pH between 1 and 10, initial aqueous silica concentration of 200-1250 ppm, experimental duration of seconds to months, ionic strengths between 0 and 4 molal and temperatures of 2-170°C. However, the reaction rates of these previous studies have been reported using various mathematical forms, i.e. forms of a rate equation. The results can, therefore, not be directly compared with each other nor

used to predict the rate of $\text{SiO}_{2(aq)}$ polymerisation and hence initial AM silica scaling potential over a wide range of temperature and water composition.

Table 4 Summary of previous experimentally measured aqueous silica polymerisation rates

Temp. (°C)	pH range	initial $\text{SiO}_{2(aq)}$	Ionic strength	Experimental duration	References
		ppm	molal		
2	1-6	6000	low	170h	Alexander (1954)
25	7-10	200-900		16h	Goto (1956)
22.3	7-10	200-900		60s	Okamoto et al. (1957)
30	0.5-9	400-1400		7h	Baumann (1959)
0-100	3-10	500-800		5h	Kitahara (1960)
25-45	8.5	300		200h	Bishop and Bear (1972)
50-120	7.8-8.7	500-1000		1000h	Rothbaum and Wilson (1977)
75-105	4.5-6.5	700-1200	<1.55	22h	Makrides et al. (1980)
5-180	7-8	300-1420	dilute	2400h	Rothbaum and Rhode (1979)
25-95	4.5-8.5	400-1000			Peck and Axtmann (1979)
60-120	5-7	500-800	0.09-1; 4	<10m	Bohlmann et al. (1980)
25	7	1000	<0.1	48h	Crerar et al. (1981)
50-100	2.5-8	500-1200	0.07	60-90m	Weres et al. (1981)
25-50	4-8	up to 300?	0-1	700-6000m	Fleming (1986)
80-150	3-9	500-600		25d	Carroll et al. (1998)
90-170	5-10	650-1000	0.2	<40h	Gallup et al. (2003)
25	3-11	250-1250	0.01-0.24	96h; 117d	Icopini et al. (2005)
25	3-7	250-1250	0.01; 0.24	277h	Conrad et al. (2007)
19-80	2.18-9.65	300-800	0.01-0.5	<800d	Gunnarsson and Arnórsson (2008)
25-90	5-8	600	0.4	<9h	Dixit et al. (2016)

The main purpose of WP4 D4.1 was to obtain such a rate equation that can be utilised for prediction of AM silica scaling in geothermal installations, for example using flow assurance simulations. Following the proposed mechanism of $\text{SiO}_{2(aq)}$ polymerisation described above, $\text{SiO}_{2(aq)}$ polymerisation involves stepwise reactions of monomeric $\text{SiO}_{2(aq)}$ to form silica tetramers until AM-silica solubility is reached. It follows that the rate of monomeric $\text{SiO}_{2(aq)}$ decrease to form $\text{SiO}_{2(aq)}$ polymers may be described by the rate function

$$\frac{dm_{\text{SiO}_{2(aq)}}}{dt} = -k \left(m_{\text{SiO}_{2(aq)}} - m_{\text{SiO}_{2(aq),eq}} \right)^4 \quad (11)$$

where k is the overall rate constant of monomeric transformation to silica tetramers, $m_{\text{SiO}_{2(aq)}}$ is the concentration of monomeric $\text{SiO}_{2(aq)}$ (Eqn. 1) in solution and $m_{\text{SiO}_{2(aq),eq}}$ is the equilibrium concentration of $\text{SiO}_{2(aq)}$ with respect to AM-silica (Table 3). The rate constant itself may depend on solution composition and temperature.

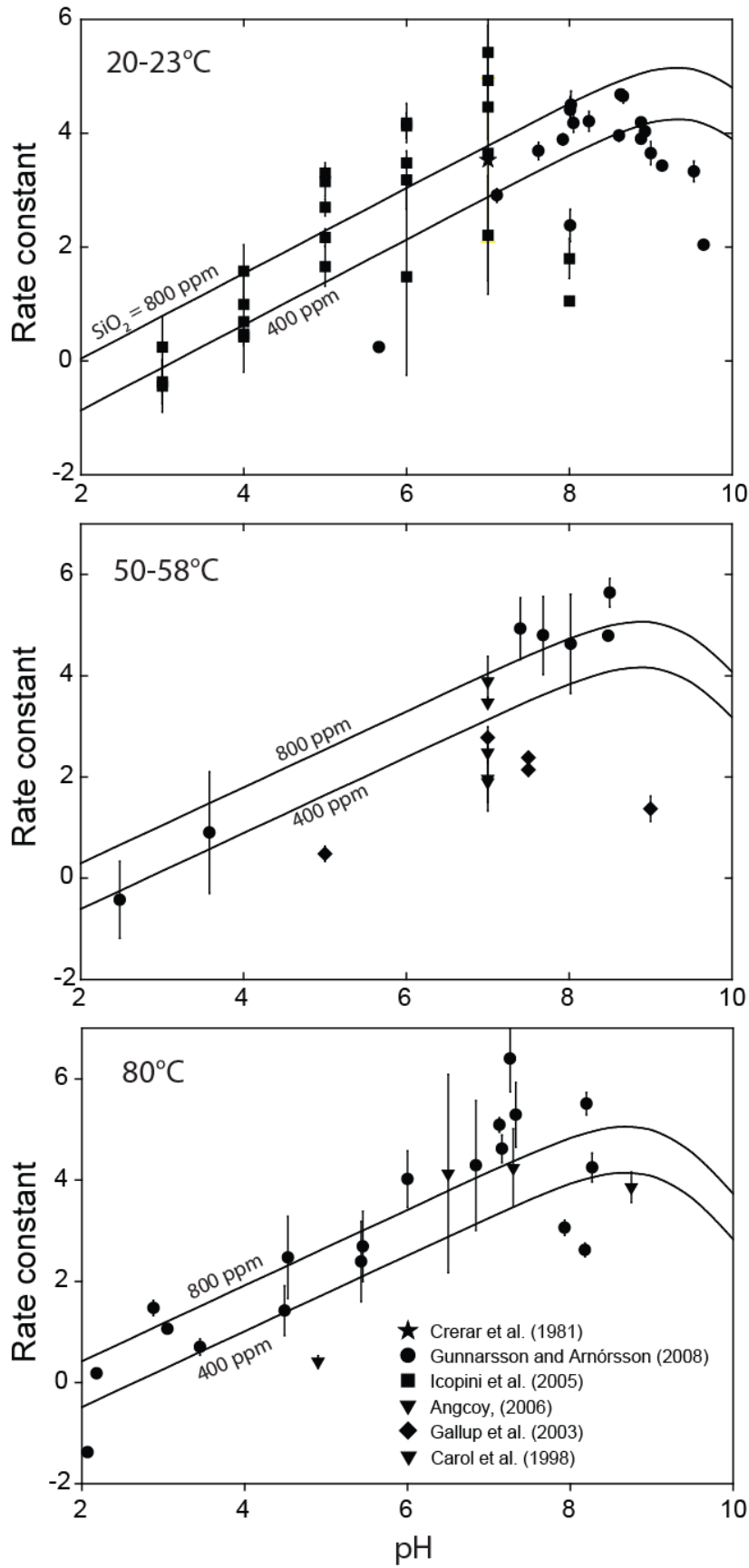


Figure 7. The comparison of the calculated rate constant based on individual experiments reported in the literature (symbols) and the rate constant fitted to the results and given by Eq. 12.

To obtain the values of the rate constant, available experimental data reported in the literature of time dependent decrease of $\text{SiO}_{2(\text{aq})}$ in solutions supersaturated with respect to AM-silica were fitted. The experimental data include the measurements reported by Crerar et al. (1981), Carroll et al. (1998), Gallup et al. (2003), Icopini et al. (2005), and Gunnarsson and Arnórsson (2008).

Based on these fits, the rate constant can be described by the equation,

$$k = A \exp(-E_a/RT) a_{\text{H}_4\text{SiO}_4, \text{aq}}^3 a_{\text{H}^+}^{-0.75} \quad (12)$$

where A is a pre-exponential constant $(3.95 \pm 1.16) \cdot 10^6$, E_a is the activation energy with value of 13.9 ± 9.8 kJ. The rate constant is valid at temperatures of ~ 20 - 80°C and pH between ~ 3 and 10. The rate constant depends on activity of H^+ , i.e. $a_{\text{H}^+} = 10^{-\text{pH}}$, possibly related to the influence of H^+ and OH^- to break $\text{Si}-\text{OH}$ and $\text{SiO}-\text{H}$ bonds needed to form linear silica polymers. The rate constant further depends on the initial concentration of $\text{H}_4\text{SiO}_{4(\text{aq})}$ that relates to the availability $\text{H}_4\text{SiO}_{4(\text{aq})}$ (or H_3SiO_4^-) for polymerisation where $a_{\text{H}_4\text{SiO}_4, \text{aq}} = m_{\text{SiO}_{2(\text{aq})}} / (1 + K_1/a_{\text{H}^+} \cdot \gamma_{\pm})$ and K_1 is the first ionisation constant of $\text{H}_4\text{SiO}_{4(\text{aq})}$ (Eq. 1, Table 3) and γ_{\pm} is the activity coefficient of a singly charged ion that can be calculated using the Davis equation.

The rate constant (and rate) of $\text{SiO}_{2(\text{aq})}$ polymerisation is observed to be a function of pH, increasing from low pH values to a maximum at pH of ~ 8 - 9 where it starts to decrease again with increasing pH (Figure 7). This trend is predicted by theoretical calculations and it is considered to be related to the availability of $\text{H}_4\text{SiO}_{4(\text{aq})}$ and H_3SiO_4^- (Zhang et al., 2011; Ciantar et al. 2015).

The rate constants derived by fitting of individual experiments reported in the literature are compared with the calculated rate constants using Eq. 12 in Figures 7 and 8. A reasonably good comparison is observed given the large spread and often large uncertainties of the experimentally derived rate constants.

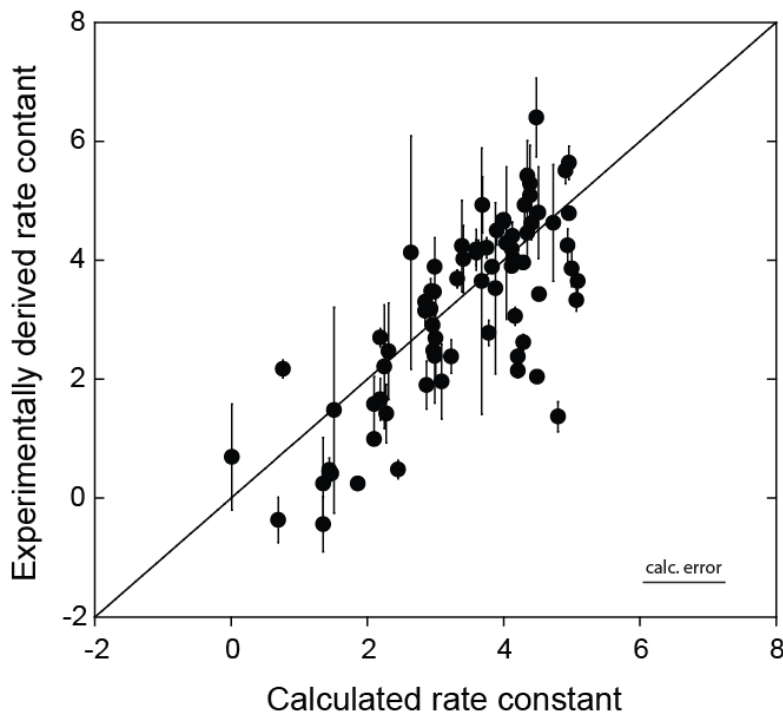


Figure 8. The comparison of experimentally derived rate constants (in $\text{mol}^{-3}\text{s}^{-1}$) and the calculated rate constants according to Eq. 12.

Integration of Eq. 11 from time 1 to 2 (Δt) can be used to calculate the concentration change of $\text{SiO}_{2(\text{aq})}$ with time, i.e.:

$$m_{SiO_2(aq)} = \frac{1}{\sqrt[3]{3k\Delta t + 1/(m_{SiO_2(aq)}^0 - m_{SiO_2(aq),eq})}} + m_{SiO_2(aq),eq} \quad (13)$$

where $m_{SiO_2(aq)}^0$ and $m_{SiO_2(aq),eq}$ are the initial $SiO_2(aq)$ concentration at $t = 0$ and equilibrium concentration with respect to AM silica, respectively. Examples of the calculated decrease in $SiO_2(aq)$ concentration to form polymeric silica are shown in Figure 9. Note that the initial and potential silica scaling formation from solution equals the difference in the calculated $SiO_2(aq)$ concentration at time t and $t=0$. The volume of the scale can be calculated based on the density of AM silica. As observed in Figure 9, the rate of polymerisation is usually insignificant within the first seconds to ~1-5 minutes. At low pH the rate continues to be slow and hence silica polymerisation and potential AM silica scaling is insignificant within hours to days. At neutral to mildly alkaline conditions (pH 7-8) the $SiO_2(aq)$ polymerisation is much faster and occurs within <1-100 minutes depending on the exact conditions like initial $SiO_2(aq)$ concentration and temperature. At more alkaline pH the polymerisation rate decreases again as well as the mass of $SiO_2(aq)$ polymerised due to decrease of the rate constant and increasing AM silica solubility with increasing pH. The silica polymerisation rates decrease with decreasing temperature, however, the mass of silica polymers formed increases with decreasing temperature as the solubility of AM silica decreases with decreasing temperature.

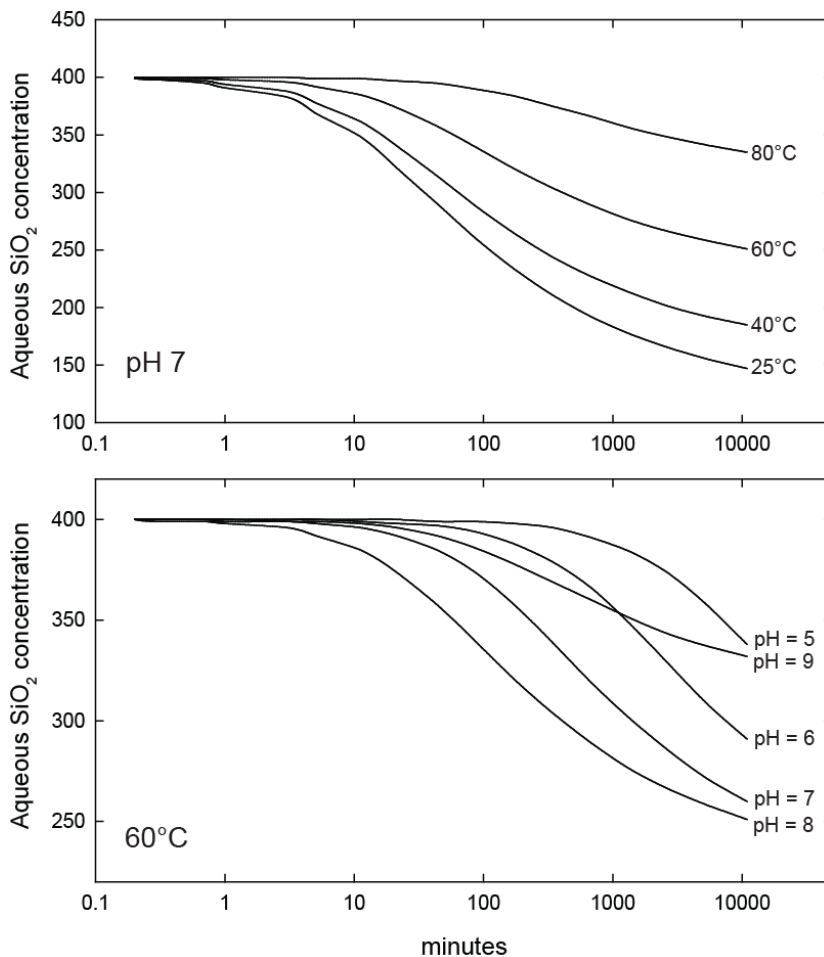


Figure 9. The calculated decrease in aqueous silica concentration ($SiO_2(aq)$) with time for silica supersaturated solutions as a function of temperature at pH 7 (above) and pH 5-9 at 60°C (below) using the rate constant given by Eq. 12. The amount of silica polymers formed is the difference between the initial aqueous silica concentration in solution and the aqueous silica concentration at a particular time. Note that silica polymerisation seems to be insignificant for the above conditions for the first 1-10 minutes but becomes significant at low temperatures and pH >7 after ~1-10 minutes.

6 TEST OF SILICA POLYMERISATION UNDER GEOTHERMAL RELEVANT CONDITIONS

6.1 Overview

In order to validate the rate equation for initial $\text{SiO}_{2(\text{aq})}$ polymerisation and potential AM silica scale formation, experimental tests were conducted to simulate the $\text{SiO}_{2(\text{aq})}$ polymerisation upon cooling of geothermal fluids representing three geothermal fields: Kizildere (Turkey), Nesjavellir (Iceland) and Hellisheiði (Iceland). The chemical composition of typical borehole fluids, reservoir fluids and re-injection fluids at these three fields are summarised in Tables 5-7.

6.2 Geothermal fields and scaling issues

6.2.1 Kizildere

Table 5 Geothermal fluid composition at Kizildere (Turkey). Reservoir fluids were calculated using the WATCH program (Bjarnason, 2010)

Sample ID	Average well fluid	Reservoir fluid	Re-injection fluid at Kizildere II
t°C	178	235	104
P (bar)	8.6		
<i>Liquid phase (ppm)</i>			
pH/°C	7.77/21	6.31/235	9.77/23
SiO ₂	470	404	451
B	22.8	19.6	24.5
Na	1197	1030	1335
K	145	125	156
Ca	4.58	3.94	4.75
Mg	0.076	0.065	0.03
Fe	0.027	0.023	0.02
Al	1.16	1	0.79
CO ₂	1576	19610	1053
Cl	109	93.8	111
F	33.1	28.5	27.5
SO ₄	802	690	944
H ₂ S	0.31	7.95	
<i>Vapor phase (mmol/kg condensate)</i>			
CO ₂	131123		
H ₂ S	55.1		
H ₂	0.085		
N ₂	485		
Ar	141		
CH ₄	196		
<i>Mineral saturation index (SI)</i>			
AM silica	-0.3	-0.48	-0.15
Calcite	1.41	0.62	1.01

Kizildere was the first geothermal field explored for electricity production in Turkey, starting in the 1960s. Today, the Kizildere geothermal plant operated by Zorlu Energy Inc. comprises of three power plants with a total installed capacity of 260 MWe: the Kizildere-I (15 MW_e), Kizildere-II (80 MW_e), and Kizildere-III (165 MW_e). The Kizildere production fluid is discharged from 1550-2872 m depths with typical reservoir temperatures of ~240-260°C (Şimşek, 2015). The waters are mainly alkaline bicarbonate with the total dissolved solids (TDS) of ~4500-6000 ppm (Şimşek, 2015). Stable isotope signature confirms meteoric origin of the thermal waters and

its deep circulation within the metamorphic hot rock complexes (Şimşek et al., 2000; Şimşek, 2003). The NCG (non-condensable gases dominated by CO₂) concentration in the deep fluid is high ranging from 1.5 to 3 wt%.

The elevated CO₂ concentrations in the fluids causes extensive calcium carbonate scale in boreholes that discharge the deep parts of the reservoir causing an annual drop in production by up to 40% (Şimşek, 2015). During the steam flashing upon the geothermal fluid utilisation the concentration of dissolved conservative elements and pH increases resulting in formation of microcrystalline CaCO₃, SrCO₃, MgCO₃, SiO₂ and traces of Al, Fe, and K have also been observed (Lindal and Kristmannsdóttir, 1989). The pH of the brine increases along the production flow line starting at about 7.5 at a wellhead followed by an increase to about 8 after separation at high pressure (HP) separators. Further separation increases the pH to about 9.5 after IP (intermediate pressure) separation and to ≥9.7 after the LPS (low pressure) separation (Şengün and Halaçoğlu, 2019). About 90% of initial Ca is precipitated in the wells before the fluid reaches the surface. Scaling has been minimised by controlling the wellhead pressure, assisted by periodic and mechanical removal. Inhibitors have also been used to prevent scaling since 2009 (Halkidir et al., 2013). If inhibitor treatment is not performed CaCO₃ and AM silica deposition starts at first production point in the Kizildere-II multi-flash system. In addition, Al-Mg-bearing silicate scales are observed in the sampling port in an injection line. To prevent their precipitation, novel types of inhibitors and inhibitor injection locations have been tested (Şengün and Halaçoğlu, 2019). At present, there is no major engineering problem with silica precipitation.

The AM silica potential at the Kizildere-II where heat exchangers and geothermal brines <100°C are utilised will be tested as a part of GeoSmart WP4. The re-injection water temperature is 104°C with a pH of 9.77/23°C. The concentration of aqueous silica in the water is 451 ppm and it is slightly supersaturated with respect to AM silica. Further decrease in utilisation temperatures may therefore cause AM silica polymerisation and silica scaling.

6.2.2 Nesjavellir

The Nesjavellir power plant is a combined geothermal heat and power plant (CHP) generating electricity and hot water for district heating. The thermal plant was commissioned in 1990 and its current capacity is estimated to be 290 MW_t and 120 MW_e. The main reservoirs of the system are at ~1000-1500 m depth with temperatures of ~260-300 °C. The reservoir fluids are dilute with chloride (Cl) concentration of 70-200 ppm, have neutral to mildly alkaline pH and are of meteoric water origin (Stefánsson et al., 2017).

The production of thermal water for direct use at the Nesjavellir requires utilisation temperatures at <100°C. As the aqueous silica concentrations in the brines are high (>600 ppm) such utilisation may potentially cause severe silica scaling issues. Initially, brines from the Nesjavellir were disposed of on the surface into a stream near the power station and condensed steam was injected into shallow boreholes. To reduce wastewater surface disposal, injection tests were performed with a mixture of separated water (30%) and condensed steam (70%) at temperatures of 40°C. However, with time the fluid flow in the re-injection borehole decreased by >50% due to silica scaling (Gíslason, 1995). Thereafter, further re-injection boreholes were drilled and experimental tests on silica scaling were conducted to better optimise re-injection conditions and minimise silica scaling (Gunnarsson et al. 2002; 2010). The results revealed that ageing of the brine for two hours at 80°C reduced considerably the concentration of SiO_{2(aq)} prior to re-injection and as a result it lowers the AM silica scaling potential of the waters within the re-injection boreholes themselves (Gunnarsson et al. 2002; 2010). In 2004 a 649 m³ retention tank was built at the power station to retain about 90 l/s of 80°C brines for 2 hours to allow SiO_{2(aq)} polymerisation and scaling to occur prior to re-injection. Later studies suggested that mixing of the brines with condensed steam after the retention tank further reduces silica scaling in re-injection wells due to reduced rates at low pH and SiO_{2(aq)} dilution. Today, the re-injection fluids at Nesjavellir at ~80-90°C consist of brines and condensed steam containing 351 ppm SiO_{2(aq)} and pH of 8.69/23°C.

Table 6 Geothermal fluid composition at Nesjavellir (Iceland). Reservoir fluids were calculated using the WATCH program (Bjarnason, 2010)

Sample ID	NJ-14	Reservoir fluid	Re-injection fluid
t°C	206	274	80
P (bar)	16.5		
Enthalpy (kJ/kg)	1198		
<i>Liquid phase (ppm)</i>			
pH/°C	8.84/17	7.12/274	8.69/23
SiO ₂	695	577	351
Na	183	152	85.5
K	34.4	28.5	17
Ca	0.436	0.36	0.19
Mg	0.007	0.001	0.02
Fe	0.009	0.003	0.05
Al	1.67	1.38	1.29
B	1.73	1.43	1.04
CO ₂	14	321	14.8
Cl	212	176	86.3
F	1.26	1.05	
SO ₄	15.6	12.9	15.6
H ₂ S	32.2	60.4	42.8
<i>Vapor phase (mmol/kg condensate)</i>			
CO ₂	41.1		
H ₂ S	5.79		
H ₂	1.73		
N ₂	0.81		
Ar	n.a.		
CH ₄	0.07		
<i>Mineral saturation index (SI)</i>			
AM silica	-0.180	-0.38	-0.02
Calcite	-0.74	-0.16	-3.60

6.2.3 Hellisheiði

The Hellisheiði geothermal power plant is a flash steam and CPH plant and it is the largest geothermal power plant in Iceland. The reservoir fluids are extracted from ~1000-2200 m depth with temperatures of ~250-300°C. Today, the production capacity is 303 MW_e and 133 MW_{th}. The reservoir fluids at Hellisheiði are dilute with chlorine concentrations <500 ppm, neutral to mildly alkaline pH and of local meteoric water source (Stefánsson et al., 2017).

The SiO_{2(aq)} concentrations in the brines at Hellisheiði power station are high, ~700-800 ppm. After the production well, the high temperature geothermal fluid is separated at 9 bar-a. Most of the brine (separated liquid) goes through a second LP separator where it boils further to 2 bar-a. After this, the 120°C brine is further utilised by flushing through heat exchangers to produce 88°C water for direct use (Sigfússon and Gunnarsson, 2011). Flushing at the LP boiler substantially increases the supersaturation of AM silica (Gunnarsson et al., 2010). To prevent silica scaling in the re-injection boreholes, the brines are retained in a ~3.3 km long pipe where the SiO_{2(aq)} is allowed to polymerise (Sigfússon and Gunnarsson, 2011). To further prevent AM silica scaling the brine is mixed with condensed steam to decrease the re-injection fluid pH and hence decrease SiO_{2(aq)} polymerisation rate and decrease SiO_{2(aq)} concentration by dilution (Gunnarsson et al., 2010; Sigfússon and Gunnarsson, 2011).

Table 7 Geothermal fluid composition at Hellisheiði (Iceland). Reservoir fluids were calculated using the WATCH program (Bjarnason, 2010)

Sample	HE-15	Reservoir fluid	Re-injection fluid
t°C	179	268	60
P (bar)	9.8		
Enthalpy (kJ/kg)	1597		
<i>Liquid phase (ppm)</i>			
pH/°C	8.79/20	6.72/268	7.61/22
SiO ₂	684	548	512
Na	182	146	143
K	30	24.03	25.7
Ca	0.49	0.39	0.45
Mg	0.002	0.002	< 0.05
Fe	0.008	0.007	< 0.05
Al	1.56	1.25	1.21
B	1.13	0.905	0.806
CO ₂	16.4	740	57.7
Cl	167	134	139
F	1.07	0.857	
SO ₄	9.6	7.69	9.03
H ₂ S	55.5	209	201
<i>Vapor phase (mmol/kg condensate)</i>			
CO ₂	83		
H ₂ S	24.2		
H ₂	9.3		
N ₂	1.99		
Ar	0.031		
CH ₄	0.207		
<i>Mineral saturation index (SI)^c</i>			
AM silica	-0.09	-0.39	0.38
Calcite	-0.84	-0.47	-2.33

6.3 Experimental tests

6.3.1 Overview

The SiO_{2(aq)} polymerisation upon cooling of geothermal fluids and re-injection fluids with similar composition to those observed at Kizildere, Nesjavellir and Hellisheiði was experimentally determined in the laboratory and the results compared with the calculated SiO_{2(aq)} polymerisation rate calculated based on Eq. 11. At Kizildere, the well liquids have typical pH of 7.8 and SiO_{2(aq)} concentration of 470 ppm whereas re-injection fluids have pH of 9.8, SiO_{2(aq)} concentration of 450 ppm and re-injection temperature of 104°C. The tests were therefore carried out at SiO_{2(aq)} concentration of ~450-500 ppm, pH between 7.3 and 9.3 and temperatures <100°C (40 and 70°C).

At Nesjavellir, typical well fluids have SiO_{2(aq)} concentration between 600-1200 ppm with pH of ~8.5-9 whereas current re-injection fluids have been diluted by condensed steam and have SiO_{2(aq)} concentration of 350 ppm, pH of 8-9 and temperatures of ~80°C. At Hellisheiði, typical well fluids have SiO_{2(aq)} concentrations of 600-1000 ppm and pH of ~8.5-9 whereas the current re-injection fluids have somewhat lower pH and SiO_{2(aq)} concentration (pH of 7.6 and 512 ppm of SiO_{2(aq)}) due to dilution with condensed steam, and temperature between 40-80°C depending on the re-injection well. The tests for Nesjavellir and Hellisheiði were therefore carried out at 400-890 ppm SiO_{2(aq)}, pH between 7.1-8.6 and temperatures between 23 and 80°C (Tables 5-8).

Table 8 Initial experimental solutions

Exp. #	Temp. °C	pH	Initial SiO _{2(aq)} (ppm)
1	40	7.4	480
2	40	9.3	480
3	70	7.3	490
4	58	7.7	800
5	80	8.2	500
6	80	7.1	890
7	23	8.6	400

6.3.2 Methods

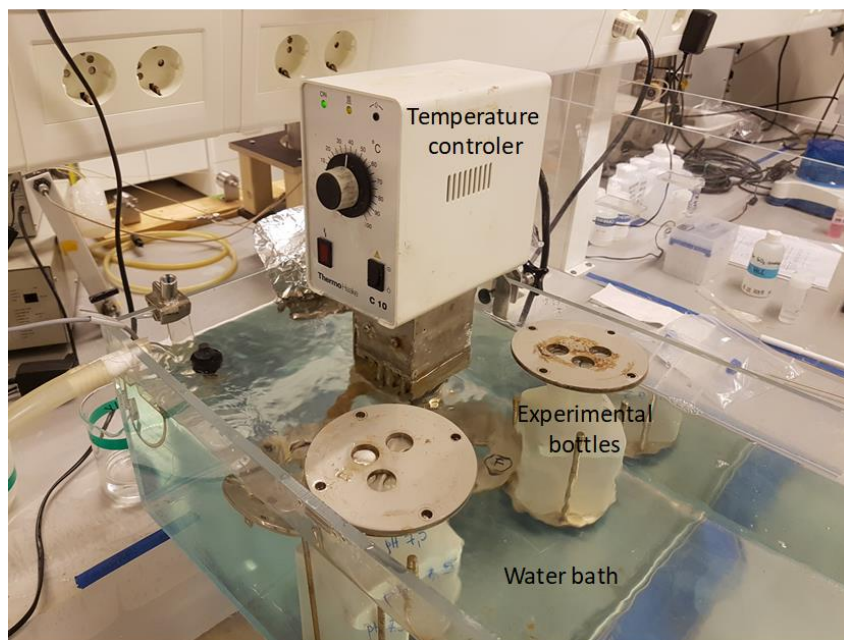


Figure 10. Experimental setup for measuring SiO_{2(aq)} polymerisation at 23, 40, 58, 70 and 80°C.

The chemical composition of the experimental solutions was produced in the laboratory to obtain similar SiO_{2(aq)} and Cl concentration as for the re-injection waters at Kizildere-II, Nesjavellir, and Hellisheiði using synthetic geothermal water. The reason for this is that untreated geothermal water cannot be used as experimental solution due to silica polymerisation upon storage. To make a synthetic geothermal solution of the desired SiO_{2(aq)} and low Cl concentration, solid silica gel (Merck) was dissolved in 0.1M NaOH solution overnight to obtain concentrated SiO_{2(aq)} solution of ~4500 ppm. The concentrated SiO_{2(aq)} solution was filtered using 0.2 µm cellulose acetate membrane and subsequently diluted to the desired SiO_{2(aq)} concentration using deionised water and the pH was adjusted using 1M HCl solution to between ~7.5 and 9.5. The pH range closely corresponds to the pH of the re-injection waters and shows possible effects of pH on the SiO_{2(aq)} polymerisation and AM silica scaling rates. The temperature of the experimental solutions was controlled by placing the bottles into a water bath with constant water temperature. The experiments were conducted in 500 ml Nalgene™ bottles (Figure 10). A number of experiments were carried out to mimic the investigated sites' reinjection conditions: experiments 1-3 to mimic the Kizildere re-injection conditions whereas experiments 4-7 to mimic the Nesjavellir and Hellisheiði reinjection of brines with 800 ppm of SiO_{2(aq)} and diluted brines with 500 of ppm SiO₂. At fixed time intervals, samples were collected for determination of monomeric SiO_{2(aq)} concentrations in solution. Approximately 1 ml of experimental solution was diluted in 9 ml of deionised water to which 0.04 ml of 1:1 concentrated HCl was added to prevent further SiO_{2(aq)} polymerisation upon sample storage. The monomeric SiO_{2(aq)} concentrations were subsequently determined spectrophotometrically after complexation with molybdenum blue (Eaton et al., 2005).

6.3.3 Results and discussion

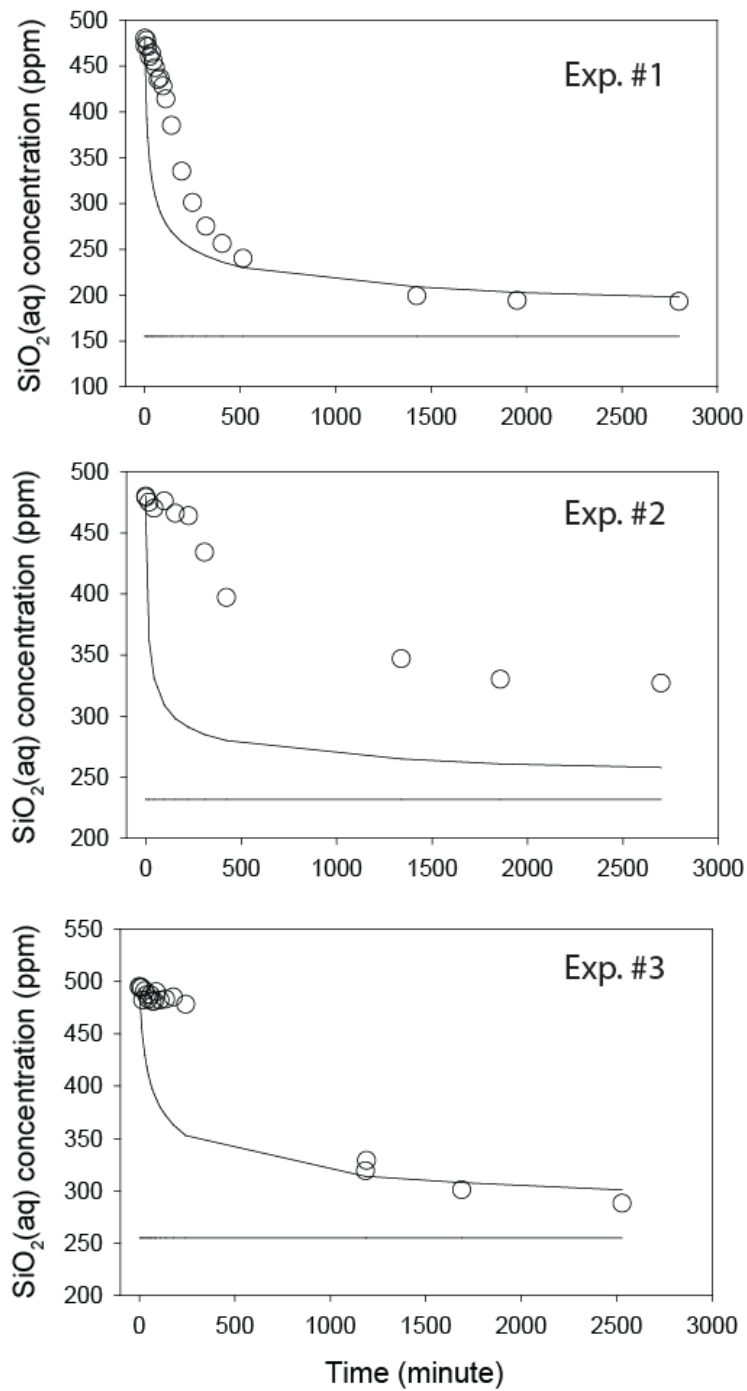


Figure 11. A comparison of the experimental and calculated rates of $\text{SiO}_2(\text{aq})$ polymerisation (Kizildere simulations).

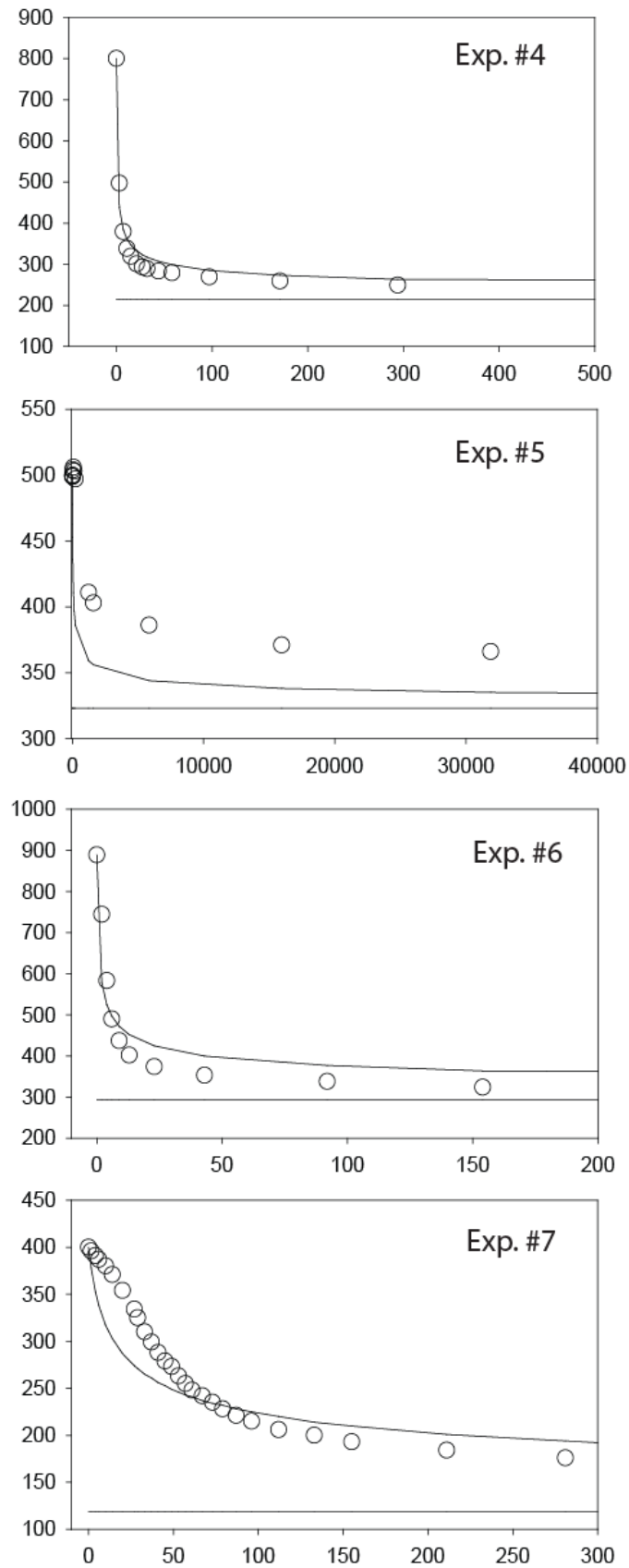


Figure 12. A comparison of the experimental and calculated rates of $\text{SiO}_{2(aq)}$ polymerisation (Nesjavellir and Hellisheiði simulations).

The results of the silica polymerisation experiments are shown in Figures 11 and 12. In all cases the monomeric $\text{SiO}_{2(\text{aq})}$ concentration was observed to decrease with time. The exact rate of $\text{SiO}_{2(\text{aq})}$ decrease and $\text{SiO}_{2(\text{aq})}$ polymerisation depended on pH, initial $\text{SiO}_{2(\text{aq})}$ concentration and temperature.

For the compositions at Kizildere, the $\text{SiO}_{2(\text{aq})}$ was observed to polymerise at 40-70°C and pH of 7.3-9.3 in minutes to hours depending on the experimental conditions. The re-injection fluids at Kizildere-II have slightly higher pH values; however these conditions were not reproduced and kept stable for the test duration due to practical difficulties.

For the compositions at Nesjavellir and Hellisheidi, $\text{SiO}_{2(\text{aq})}$ was also observed to polymerise within a few minutes at high initial $\text{SiO}_{2(\text{aq})}$ concentrations and hours at lower $\text{SiO}_{2(\text{aq})}$ concentrations; hence the rate of silica polymerisation can be greatly reduced by dilution and lowering $\text{SiO}_{2(\text{aq})}$ concentration.

The experimental results are further compared with the rate function proposed in this study (Eq. 11) in Figures 11 and 12. A reasonably good comparison is observed in all cases except at the most alkaline conditions (Exp. 2) where observed $\text{SiO}_{2(\text{aq})}$ polymerisation was much lower than predicted. However, the rate function (Eq. 11) has large errors at high pH values (>9-10) due to lack of data on experimentally derived rate constants and large differences between the experimental values.

Based on these tests it can be concluded that conductive cooling of the re-injection water at Kizildere-II to 70°C results in insignificant $\text{SiO}_{2(\text{aq})}$ polymerisation and AM silica scale formation whereas further cooling of the waters to 40°C may result in minor $\text{SiO}_{2(\text{aq})}$ polymerisation and AM silica scale formation. At pH between ~7.5 and ~9.5 and after 10 min of the reaction time ≤1% and after 60 min up to 5% of the initial SiO_2 have polymerised, respectively.

Conductive cooling of waters at Nesjavellir and Hellisheidi that contain up to 800 ppm of $\text{SiO}_{2(\text{aq})}$ and 80°C will result in significant $\text{SiO}_{2(\text{aq})}$ polymerisation within minutes or ~25% of the initial $\text{SiO}_{2(\text{aq})}$ within 10 minutes and ~40% within an hour. Further cooling will enhance the polymerisation, and >50% of the initial $\text{SiO}_{2(\text{aq})}$ will polymerise in 10 minutes at 58°C and 23°C. Upon dilution of such brines with condensed steam as practised both at Nesjavellir and Hellisheidi, the $\text{SiO}_{2(\text{aq})}$ polymerisation rates are greatly reduced. For waters with <500 ppm of $\text{SiO}_{2(\text{aq})}$ and at 80°C, ≤1% of the initial $\text{SiO}_{2(\text{aq})}$ is predicted to polymerise in 24 hours. Upon further cooling, a similar extent of polymerisation is expected as for Kizildere re-injection fluid.

7 CONCLUSIONS

The major conclusions of the work described are:

- A mathematical function has been developed that describes the rate of aqueous silica ($\text{SiO}_{2(\text{aq})}$) polymerisation in geothermal water corresponding to rate of initial AM silica scaling. It is based on reported measured $\text{SiO}_2(\text{aq})$ polymerization rates in the literature. The mathematical function is valid at 25-80°C, pH 3-10 and ionic strength $I > 0.1$ molal.
- The rate of $\text{SiO}_{2(\text{aq})}$ polymerisation and AM silica scaling is at maximum at pH ~8-9 and decreases with decreasing and increasing pH, increases with increasing temperature and initial $\text{SiO}_{2(\text{aq})}$ concentration.
- Based on the rate function and laboratory test, conductive cooling of the re-injection water at Kizildere-II to 70°C results in insignificant $\text{SiO}_{2(\text{aq})}$ polymerisation and AM silica scale formation whereas further cooling of the waters to 40°C may result in minor $\text{SiO}_{2(\text{aq})}$ polymerisation and AM silica scale formation (≤1% after 10% and 5% after 1 hour).
- Conductive cooling of waters at Nesjavellir and Hellisheidi to 80°C results in significant $\text{SiO}_{2(\text{aq})}$ polymerisation within minutes (~25% within 10 minutes and ~40% within 1 hour). Further cooling will enhance the polymerisation (>50% after 10 minutes at ~20-60°C). Upon dilution of the brines with condensed steam as practised both at Nesjavellir and Hellisheidi, the $\text{SiO}_{2(\text{aq})}$ polymerisation rates are greatly reduced. For waters with <500 ppm of $\text{SiO}_{2(\text{aq})}$ and at 80°C, ≤1% of the initial $\text{SiO}_{2(\text{aq})}$ is predicted to polymerise in 24 hours. Upon further cooling, a similar extent of polymerisation is expected as for Kizildere re-injection fluid.

REFERENCES

- Alexander G.B. (1954) The Polymerization of Monosilicic Acid. *J. Amer. Chem. Soc.* 76, 2094-2096.
- Arnórsson S., Sigurdsson S., Svavarsson H. (1982) The chemistry of geothermal waters in Iceland 1. Calculation of aqueous speciation from 0 °C to 370 °C. *Geochim. Cosmochim. Acta* 46, 1513-1532.
- Baumann H. (1959) Polymerisation und Depolymerisation der Kieselsäure unter verschiedenen Bedingungen. *Kolloid-Zeitschrift* 162, 28-35.
- Benning L.G., Waychunas G.A. (2007) Nucleation, growth, and aggregation of mineral phases: mechanisms and kinetic controls. *Kinetics of Water-Rock Interaction*. Springer, pp. 259–333.
- Bilinski H., Ingri N. (1967) A Determination of the Formation Constant of $\text{SiO}(\text{OH})_3^-$. *Acta Chem. Scand.* 21, 2503-2510.
- Bishop Jr A.D., Bear J.L. (1972) The thermodynamics and kinetics of the polymerization of silicic acid in dilute aqueous solution. *Thermochim. Acta* 3, 399-409.
- Bjarnason J.Ö. (2010) The chemical speciation program WATCH, version 2.4. Iceland GeoSurvey, Reykjavik, Iceland.
- Bohlmann E.G., Mesmer, R.E., Berlinski, (1980) Kinetics of Silica Deposition From Simulated Geothermal Brines. *Soc. Petrol. Eng. J* 20, 239-248.
- Busey R.H., Mesmer R. E. (1977) Ionization equilibria of silicic acid and polysilicate formation in aqueous sodium chloride solutions to 300°C. *Inorg. Chem.* 16, 2444-2450.
- Candelaria M. N. R., Garcia S. E., Baltazar A. D. J., Solis R. P., Cabel A.C. Jr., Nogara J. B., Reyes R. L., Jordan O. T. (1996) Methods of coping with silica deposition - the PNOX experience. *Geotherm. Res. Council Trans.* 20, 661-672.
- Carroll S., Mroczek E., Alai M., Ebert M. (1998) Amorphous silica precipitation (60 to 120°C): Comparison of laboratory and field rates. *Geochim. Cosmochim. Acta* 62, 1379–1396.
- Chen C.-A. T., Marshall W. (1982) Amorphous silica solubilities IV. Behavior in pure water and aqueous sodium chloride, sodium sulfate, magnesium chloride, and magnesium sulfate up to 350°C. *Geochim. Cosmochim. Acta* 46, 279–287.
- Ciantar M., Mellot-Draznieks C., Nieto-Draghi C. (2015) A kinetic Monte Carlo simulation study of synthesis variables and diffusion coefficients in early stages of silicate oligomerization. *J. Phys. Chem.* 119, 28871–28884.
- Conrad C.F., Icopini G.A., Yasuhara H., Bandstra J.Z., Brantley S.L., Heaney P.J. (2007) Modeling the kinetics of silica nanocolloid formation and precipitation in geologically relevant aqueous solutions. *Geochim. Cosmochim. Acta* 71, 531-542.
- Crerar D. A., Anderson G. M. (1971) Solubility and solvation reactions of quartz in dilute hydrothermal solutions. *Chem. Geol.* 8, 107–122.
- Crerar D.A., Axtmann E.V., Axtmann R.C. (1981) Growth and ripening of silica polymers in aqueous solutions. *Geochim. Cosmochim. Acta* 45, 1259-1266.
- Dixit C., Bernard M.-L., Sanjuan B., André L., Gaspard S. (2016) Experimental study on the kinetics of silica polymerization during cooling of the Bouillante geothermal fluid (Guadeloupe, French West Indies). *Chem. Geol.* 442, 97-112.
- Eaton A.D., Clesceri L.S, Rice E.W., Greenberg A.L., Franson M.A.H. (eds) (2005): Standard methods for the examination of water & wastewater, 21st Edition. *American Public Health Association*, Washington DC, 4-174
- Elmer T. H., Nordberg M. E. (1958) Solubility of silica in nitric acid solutions. *J. Amer. Ceram. Soc.* 41, 517–520.

Document: D4.1 Modelling of scaling potential of geofluids

Version: 2

Date: 28 May 2020

Fleming B.A. (1986) Kinetics of reaction between silicic acid and amorphous silica surfaces in NaCl solutions. *J. Coll. Interf. Sci.* 110, 40-64.

Gallup D. L. (1998) Investigations of organic inhibitors for silica scale control in geothermal brines. *Geothermics* 27, 485-501.

Gallup D. L., Featherstone J. L. (1985) Acidification of steam condensate for incompatibility control during mixing with geothermal brine. US Patent 4,522,728.

Gallup S.L., Sugiaman F., Capuno V., Manceau A. (2003) Laboratory investigation of silica removal from geothermal brines to control silica scaling and produce usable silicates. *Appl. Geochem.* 18, 1597–1612.

Gill J. S. (1993) Inhibition of silica-silicate deposition in industrial wastewaters. *Colloids and Surfaces A* 74, 101-106.

Gíslason G. (1995) Injection tests in NN-2, Nesjavellir Reykjavík Energy report, 8 pp.

Goto K. (1956) Effect of pH on Polymerization of Silicic Acid. *J. Phys. Chem.* 60, 1007-1008.

Greenberg S. A., Price E. W. (1957) The solubility of silica in solutions of electrolytes. *J. Phys. Chem.* 61, 1539–1541.

Greenberg S. A. (1958) The nature of the silicate species in sodium silicate solutions. *J. Am. chem. Soc.* 80, 6508 - 6511.

Gudmundsson S. R., Einarsson E. (1989) Controlled silica precipitation in geothermal brine at the Reykjanes geochemical plant. *Geothermics* 18, 105-112.

Gunnarsson I., Arnórsson S. (2000) Amorphous silica solubility and the thermodynamic properties of $\text{H}_4\text{SiO}_4^\circ$ in the range of 0° to 350°C at Psat. *Geochim. Cosmochim. Acta* 64, 2295–2307.

Gunnarsson I., Arnórsson S., Hauksson T. (2002) Nesjavellir Power Plant. Experiments to prevent silica deposition from wastewater. Science Institute Report RH-02-02, University of Iceland, 104 p.

Gunnarsson I., Ívarsson G., Sigfússon B., Thrastarson E.Ö., Gíslason G. (2010) Reducing Silica Deposition Potential in Waste Waters from Nesjavellir and Hellisheiði Power Plants, Iceland. Proc. WGC 2010 Bali, Indonesia.

Gunnarsson I., Arnórsson S. (2008) Polymerization of silica in high temperature geothermal fluids Report RH-02-08, Science Institute, Iceland Univ., 99p.

Haklıdır, F.S.T., Akin, T., Parlaktuna, Ç., Turk, D., Savaş, T., 2013. Scaling Types and Prevention and Control of Scaling in the Operation Stage in Geothermal Field: Kizildere Geothermal Field Case Study. Geological congress of Turkey.

Hemley J. J., Montoya J. W., Marinenko J. W., Luce R. W. (1980) Equilibria in the system $\text{Al}_2\text{O}_3\text{--SiO}_2\text{--H}_2\text{O}$ and some general implications for alteration/mineralization processes. *Econ. Geol.* 75, 210-228.

Hitchen S. (1935) A method for the experimental investigation of hydrothermal solutions, with notes on its application to the solubility of silica. *Trans. Inst. Min. Metall.* 44, 255–280.

Icopini G.A., Brantley S.L., Heaney P.J. (2005) Kinetics of silica oligomerization and nanocolloid formation as a function of pH and ionic strength at 25°C. *Geochim. Cosmochim. Acta* 69, 293–303.

Ingri N. (1959) Equilibrium studies of polyanions IV. Silicate ions in NaCl media. *Acta Chem. Scand.* 13, 758-775.

Kennedy G. C. (1950) A portion of the system silica–water. *Econ. Geol.* 45, 629–653.

Kitahara S. (1960) The polymerization of silicic acid obtained by the hydrothermal treatment of quartz and the solubility of amorphous silica. *Rev. Phys. Chem. Japan* 30, 131-137.

Lagerstrom G. (1959) Equilibrium studies of polyanions III. Silicate ions in NaClO, medium. *Acta. Chem. Scand.* 13, 722-736.

Lenher V. and Merrill H. B. (1917) The solubility of silica. *J. Amer. Chem. Soc.* 39, 2630–2640.

Lindal, B., Kristmannsdóttir, H. (1989). The scaling properties of the effluent water from Kizildere power station, Turkey, and recommendation for a pilot plant in view of district heating applications. *Geothermics* 18, 217–223.

Mackenzie F. T. and Gees R. (1971) Quartz: Synthesis at earth surface conditions. *Science* 173, 533–535.

Makrides A.C., Turner M., Slaughter J. (1980) Condensation of silica from supersaturated silicic acid solutions. *J. Coll. Interf. Sci.* 73, 345-367.

Marshall W. (1980) Amorphous silica solubilities—I. Behavior in aqueous sodium nitrate solutions; 25°–300°C, 0–6 molal. *Geochim. Cosmochim. Acta* 44, 907–913.

Morey G. W., Fournier R. O., and Rowe J. J. (1962) The solubility of quartz in water in the temperature interval from 25 to 300°C. *Geochim. Cosmochim. Acta* 26, 1029–1043.

Morey G. W., Fournier R. O., and Rowe J. J. (1964) The solubility of amorphous silica at 25°C. *J. Geophys. Res.* 69, 1995–2002.

Naumov G.B., Ryzhenko B.N., Khodakovskiy I.L. (1971) Handbook of thermodynamic data (translation of Russian report)

Okamoto G., Okura T., Goto K. (1957) Properties of silica in water. *Geochim. Cosmochim. Acta* 12, 123-132.

Peck L. B., Axtmann R. C. (1979) A theoretical model of the polymerization of silica in aqueous media. *Int. Symp. on Oilfield and Geothermal Chemistry, Soc. Pet. Eng. A.I.M.E. Trans.*, pp. 239–247.

Rimstidt J. D. (1997) Quartz solubility at low temperatures. *Geochim. Cosmochim. Acta* 61, 2553–2558.

Rothbaum H. P., Wilson R. D. (1977) Effect of temperature and concentration on the rate of polymerization of silica in geothermal waters. In *Geochemistry 1977*. New Zealand Dept. Sci. Ind. Res. Bull.

Rothbaum H.P., Rohde A.G. (1979) Kinetics of silica polymerization and deposition from dilute solutions between 5 and 180°C. *J. Coll. Interf. Sci.* 71, 533-559.

Ryzenko B. N. (1967) Determination of hydrolysis of sodium silicate and calculation of dissociation constants of orthosilicic acid at elevated temperatures. *Geochem. Int.* 4, 99-107.

Schwarz, R. and Muller, W. D. (1958) Zur Kenntnis der Kieselsäuren. XIV. Die wasserlösliche monokieselsäure. *Z. Anorg. Allg. Chem.* 296, 273-279.

Şengün, R., Halaçoğlu, U., 2019. Kizildere geothermal field geochemistry report. ZOREN Copyright © 2019-2023, GeoSmart Consortium.

Seward T.M. (1974) Determination of the first ionization constant of silicic acid from quartz solubility in borate buffer solutions to 350°C. *Geochim. Cosmochim. Acta* 38, 1651-1664.

Siever R. (1962) Silica solubility 0–200°C, and the diagenesis of siliceous sediments. *J. Geol.* 70, 127–150.

Sigfusson B., Gunnarsson I. (2011) Scaling prevention experiments in the Hellisheidi power plant, Iceland. *Proc. 36th Workshop Geotherm. Res. Eng., Stanford*. SGP-TR-191

Şimşek, Ş., Dogdu, M.S., Akan, B., Yildirim, N., 2000. Chemical and isotopic survey of geothermal reservoirs in Western Anatolia, Turkey. *Proceedings World Geothermal Congress, Japan*, pp. 1765–1770.

Şimşek, Ş., 2003. Hydrogeological and isotopic survey of geothermal fields in the Büyük Menderes graben, Turkey. *Geothermics* 32, 669-678.

Şimşek, Ş., 2015. Geothermal developments in the world and Turkey. *Proceedings of Geothermal Resources Conference, Ankara-Turkey, 4–6 November, 2015 (2015)*, pp. 1-19.

Sjöberg S., Nordin A., Ingri N. (1981) Equilibrium and structural studies of silicon(IV) and aluminium(III) in aqueous solution. II. Formation constants for the monosilicate ions $\text{SiO}(\text{OH})_3^-$ and $\text{SiO}_2(\text{OH})_2^{2-}$. A precision study at 25°C in a simplified seawater medium. *Marine Chem.* 10, 521-532.

Document: D4.1 Modelling of scaling potential of geofluids

Version: 2

Date: 28 May 2020

Stefansson A., Hilton D.R., Sveinbjörnsdóttir Á.E., Torssander P., Heinemeier J., Barnes J.D., Ono S., Halldorsson S.A., Fiebig J., Arnorsson S. (2017) Isotope systematics of Icelandic thermal fluids. *J. Volcanol. Geotherm. Res.* 337, 146-164.

Sugita H., Bando Y., Nakamura M. (1998) Removal of silica from geothermal brine by seeding method using silica gel. *J. Chem. Eng. Japan* 31, 150-152.

Sugita H., Kato K., Ueda A., Matsunaga I., Sakurai Y., Yasuda K., Bando Y., Nakamura M. (1999) Field tests on silica removal from geothermal brines in Sumikawa and Onuma geothermal areas. *J. Chem. Eng. Japan* 32, 696-700.

Tobler D.J., Benning L.G. (2013) In situ and time resolved nucleation and growth of silica nanoparticles forming under simulated geothermal conditions. *Geochim. Cosmochim. Acta* 114, 156–168.

Tobler D.J., Shaw S., Benning L.G. (2009) Quantification of initial steps of nucleation and growth of silica nanoparticles: An in-situ SAXS and DLS study. *Geochim. Cosmochim. Acta* 73, 5377-5393.

Ueda A., Kato K., Abe K., Mogi K., Furukawa T., Ishimi K. (2000) Recovery of silica from the Sumikawa geothermal fluids by addition of cationic reagents. *J. Geoth. Res. Soc. Jnp.* 22, 249-258.

Ueda A., Kato K., Mogi K., Mroczek E., Thain I. A. (2003) Silica removal from Mokai, New Zealand, geothermal brine by treatment with lime and a cationic precipitant. *Geothermics* 32, 47-61.

van den Heuvel D.B., Gunnlaugsson E., Gunnarsson I., Stawski T.M., Peacock C.L., Benning L. G. (2018) Understanding amorphous silica scaling under well-constrained conditions inside geothermal pipelines. *Geothermics* 76, 231–241.

Van Lier, J. H., de Bruyn, P. L. and Overbeek, Th. G. (1960) The solubility of quartz. *J. Phys. Chem.* 64, 1675 - 1682.

Vilim J. (1961) Berechnung der Dissoziations konstanten KI aus der Löslichkeitsmessung von Kieselsäure in sattdampft bei verschiedener Wasseralkalität. *Collect. Czech. Chem. Commun.* 26, 1268-1273.

Wen L., Xu J., Yang Q., Zhang F., Li F., Zhang L. (2020) Gelation process of nanosilica sol and its mechanism: Molecular dynamics simulation. *Chem. Eng. Sci.* 216, 115538.

Weres O., Yee A., Tsao L. (1981) Kinetics of silica polymerization. *J. Coll. Interf. Sci.* 84, 379-402.

Yanagase T., Suginochara Y. and Yanagase K. (1970) The properties of scales and methods to prevent them. *Geothermics (special issue 2)*, 1619-1623.

Zhang X-Q, Trinh T.T., van Santen R.A., Jansen A.P.J. (2011) Mechanism of the initial stage of silicate oligomerization. *J. Am. Chem. Soc.* 133, 6613–6625.